Progress In Electromagnetics Research, PIER 84, 105–122, 2008

BEAM COMPRESSED SYSTEM FOR MEASURING INHOMOGENEITY AND IRREGULARITY OF DIELECTRIC PLATE WITH HIGHER SPATIAL RESOLUTION POWER

L. Z. You †, **W. B. Dou, C. Qian, and Z. X. Wang**

State Key Lab of Millimeter Waves
Southeast University
Nanjing 210096, P. R. China

Abstract—The measurement of inhomogeneity and irregularity of dielectric plate requires metering equipments with high spatial resolution power and contactless method. As we know, a measurement system with thin beam has high spatial resolution power. In this paper, a beam compressed system (BCS) is proposed to improve the spatial resolution power for measuring inhomogeneity and irregularity of dielectric plate at millimeter wave band. The beam shape of the BCS has to be carefully designed to achieve a very thin shape which has to be constant over a long range. The BCS can be applied to detect inhomogeneity and irregularity of a dielectric plate from cell to cell with its thin beam. Simulations with FDTD and FEM and experiments are carried out to confirm the performance of the designed BCS, both simulation and experimental results have good agreement. And the images of the permittivity or thickness variance of dielectric plate are given to demonstrate the advantages of the BCS over traditional Gaussian beam measuring method.

1. INTRODUCTION

Measuring the material characteristics, for instance, thickness and dielectric constant is important for the production of millimeter wave circuits on semiconductor, quasi optical lens or for radome material. Design of integrated circuits on dielectric plate needs the information of permittivity exactly at millimeter wavelengths. Permittivity is also to be known accurately in designing radome, which is generally in

† Also with Radar and Avionics Institute of AVIC, WuXi 214063, P. R. China

non-planar form. In millimeter wave focal imaging system, the lens used is electric larger, for example, its diameter will be or exceed 100 wavelengths. However, there may be some inhomogeneity of permittivity in the lens material. In order to get good imaging performance, the permittivity of the lens material needs to be know from cell to cell so as emendation to the lens can be done. In microwave band, the measurement of permittivity of dielectric material is done by using closed cavity or waveguide, which requires the dielectric material to be shaped to insert into the closed cavity or waveguide. But at millimeter wave band, it is hard to machine the sample to fit the cavity or waveguide with negligible air gaps, which gives limitation to the accuracy of measurements. Quasi-optical techniques, including open cavity and free space method, have been developed to measure permittivity of dielectric material since 1980's [1–6]. These techniques are based on Gaussian beam theory. For open cavity method, a Gaussian beam standing wave is established in the open cavity, the dielectric plate to be measured is placed at the beam waist location. For free space method, a Gaussian beam traveling wave is established by beam waveguide; the dielectric plate is also placed at the beam waist location. A method, which combine open cavity method and free space method, is proposed to measure a dielectric material with permittivity approaching to that of air [7]. Therefore, the spatial resolution power of the measurement techniques depends on the size of the beam waist. It has been proved that the beam waist radius must be greater than one wavelength or at least equal one wavelength so as the properties of Gaussian beam can be kept [8]. In measurements, the dielectric plate must have large size in planar form so as the diffraction at the plate edges can be neglected. Generally the sample dielectric plate should be three times larger than the radius of the beam waist size. Furthermore, when the dielectric plate is inhomogeneous or irregular from cell to cell, this spatial resolution power can not meet the requirement for the limitation of the beam waist size. If a measurement system can produce a thin beam, the spatial resolution power will be improved, and the size of the sample dielectric plate can be reduced. On the other hand, the thin beam only need a small aperture receive antenna, so a crooked dielectric material, such as cylindrical sleeve, hemisphere or ogive radome etc. can be measured with this measurement system. To improve spatial resolution power, an improved reverse microscope system (BCS), is proposed to obtain a thin beam in this paper. It can be seen that the technique can be easily expanded to sub-millimeter waves.

On the other hand, microwave microscopy of materials is also attractive for their high spatial resolution even to nanometer scale.

It is suitable to examine physics of single crystal, ceramic and thin-film samples on micrometer or nanometer length scales [9–12]. The microwave microscopy is associated with the concept of so-called near field interactions between a source and a sample in which near-zone fields and/or evanescent waves are created and interact with the sample. In order to create a true near-zone or evanescent field in the sample, the characteristic size D of the tip used in microscopy must be small enough not only compared to the free-space wavelength λ, but also to provide $|k_s|D \ll 1$, where $k_s = \omega(\varepsilon_0\varepsilon_s\mu_0\mu_s)^{1/2}$ is the complex wave number of the material under test [12]. Furthermore, a good rule of thumb is that the tip should be held reliably at a distance h above the sample that is less than one-tenth of the tip size D [12]. It can be regarded as contact method. Such small values of D and h bring much difficulty in fabrication and measurement at millimeter waves. And the techniques mainly focus on the measurement of thin film of semiconductor circuits and may not be suitable for measuring some thick dielectric plate such as lens or radome materials due to the very short length of evanescent wave decay.

Recently, permittivity measurement based waveguide has also proceeded, but it is limited in microwave band [13]. Lens can be used to transform Gaussian beam or used as antennas in higher frequency bands [14, 15]. Scattering of Gaussian beam is also interested [16, 17]. Permittivity distribution reconstruction of dielectric object is considered in [18]. In [19] mirror is investigated for beam shaping. Extended hemispherical lens and spheric lens have been researched for their application as antenna or as imaging lens [20, 21]. In this paper a lens system combining hyperbolic lens with extended hemispherical lens are modified to measure permittivity of dielectric plate with higher spacial resolution power.

Section 2 describes the structure and operating principle of the BCS. Both finite difference time domain (FDTD) method and finite element method (FEM) are applied to verify the validity of the high spatial resolution BCS. Section 3 describes the experiments to verify the validity of the BCS. Section 4 introduces briefly the numerical extraction techniques of permittivity and thickness. In Section 5, we discuss the BCS applications in measuring inhomogeneity and irregularity of dielectric plate from cell to cell. And the images of the permittivity or thickness variance of dielectric plate are given to demonstrate the advantages of the BCS over traditional Gaussian beam measuring method. Conclusions are described in the final section.

2. DESCRIPTION OF THE MEASUREMENT SYSTEM AND SIMULATION RESULTS

Reverse-microscope system (RMS) is often used as imaging lens in far-infrared and millimeter waves imaging system [8, 22, 23]. It is composed of a hyperbolic lens and an extended hemispherical lens as shown in Fig. 1. For millimeter wave imaging, an integrated receiving antenna array is placed on the focal plane of RMS. The permittivity of extended hemispherical lens is chosen to be equal to that of integrated antenna substrate so as the trapped surface wave in the substrate can be eliminated. Further details of RMS can be found in [23]. It has been known that RMS can also reduce the central lobe size of the power distribution on focal plane. It gives us a hint to use RMS to reduce beam size, but the RMS disperses the output electromagnetic wave more sharply than the single hyperbolic lens (SHL) does. However, it is often needed that the output electromagnetic wave propagates as a thin beam so that the spatial resolution power is higher. In order to achieve this goal, a beam compressed system (BCS) (Fig. 2) is proposed and designed. A buncher lens, which can congregate the output electromagnetic wave in a small region, is placed at the right side of RMS to constitute BCS, which is just the originality of this paper. The optical paths in Fig. 2 show that the BCS can congregate the output electromagnetic wave in a small region along the wave propagating direction. If the parameters of the buncher lens are adjusted carefully, the most power of output electromagnetic wave can be restricted in a small space region as it propagates like a thin beam for a certain distance required. Fig. 3 shows the shape, material

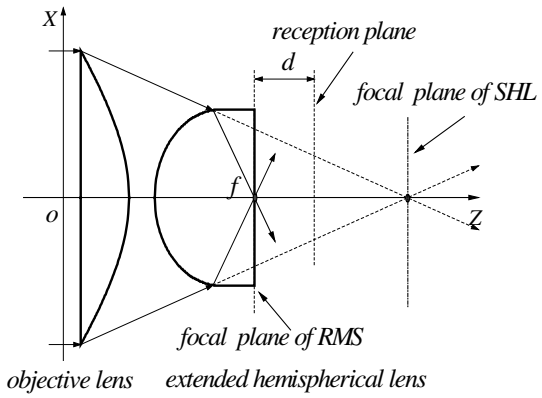

Figure 1. Configuration of RMS.

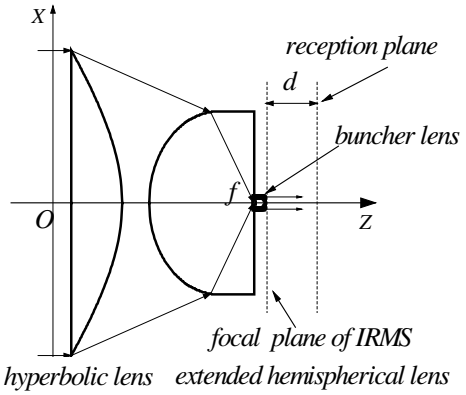

Figure 2. Configuration of BCS.

parameters and dimensions of the buncher lens designed in detail.

Here the BCS is utilized to congregate the output wave in a small region. The field distribution on the reception plane is calculated to show the congregate performance more finely. The reception plane is at a distance of d from focal plane of the RMS or BCS (as shown in Fig. 1 and Fig. 2). Simulations for the congregating performance of the RMS and BCS have been carried out using two dimensional finite difference time domain (FDTD) method and two dimensional finite element method (FEM), which are the most trusted methods. In FDTD, fields on the reception plane in time domain are recorded and then transformed into frequency domain by Fourier transform, thus the power distribution on the reception plane in frequency domain is obtained. In FEM, fields on the reception plane are recorded at each frequency in frequency sweep and then the power distribution on the reception plane in frequency domain is obtained. The FDTD method has been described in [24] and FEM in [25]. The treatment procedure has been omitted here for saving space.

Figure 4 shows the power distribution on the focal plane of RMS and BCS at frequency 37.5 GHz calculated by FEM and FDTD method with plane wave incidence. The parameters of the designed BCS are indicated in Fig. 3 and $D = 100\,\text{mm}$, $T = 21.94\,\text{mm}$, $\varepsilon_{r1} = 2.1$ (Teflon), $S = 11.67\,\text{mm}$, $R = 30\,\text{mm}$, $L = 15.43\,\text{mm}$, $Ra = 2\,\text{mm}$, $La = 3.2\,\text{mm}$, $\varepsilon_{r2} = 3.78$ (Quartz-glass). The two methods give almost the same results, which prove the validity of the simulations. Fig. 5 depicts the configuration and power distribution of a Gaussian beam, in which the $d = 0\,\text{mm}$ plane is the plane where the waist of Gaussian beam located, which is called the beam waist plane; and other reception

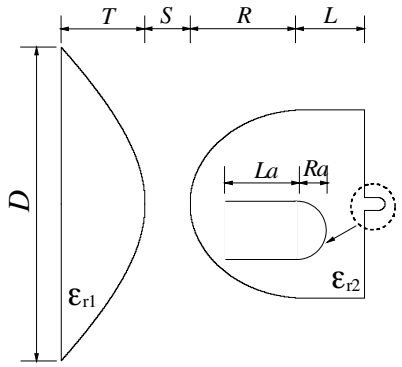

Figure 3. Parameters definition of BCS.

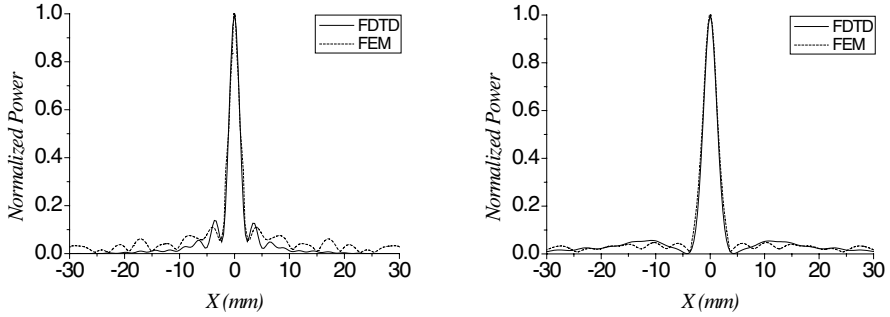

Figure 4. Power distribution on the focal plane at frequency at 37.5 GHz.

planes are at a distance of d away from the waist plane as shown in Fig. 5(a).The beam waist radius of the Gaussian beam used here is 8 mm, which equals one wavelength at the frequency 37.5 GHz. Fig. 6 shows the power distribution of RMS and BCS on the reception plane at different d values at frequency 37.5 GHz. Comparing Fig. 5(b) with Fig. 6, it can be seen that Gaussian beam has the largest beam size and BCS has the least beam size.

The half power beam width (HPBW) of Gaussian beam on the beam waist plane is about 10 mm and that of BCS on the focal plane is only 2 mm, which is less than 1/5 of the Gaussian beam as shown in Fig. 5(b) and Fig. 6(b). If the HPBW is used to stand for the spatial resolution power, the space resolution power of BCS is about 2 mm and the Gaussian beam 10 mm. That is, BCS has higher spatial resolution

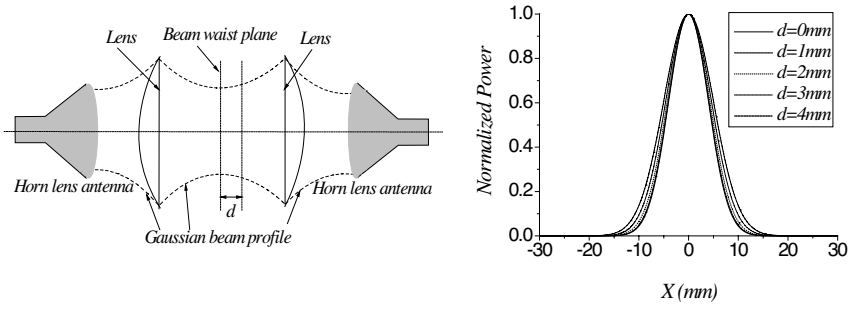

(a) Configuration (b) Power distribution on reception planes

Figure 5. Configuration and the power distribution of a Gaussian beam system at 37.5 GHz.

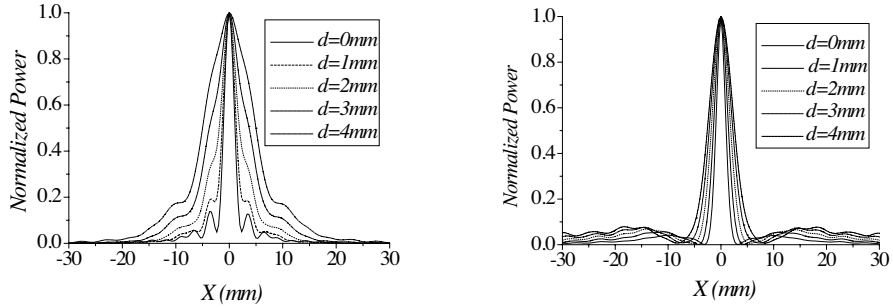

(a) RMS (b) BCS

Figure 6. Power distribution on reception planes at 37.5 GHz.

power than Gaussian beam does. Fig. 7 gives the contour diagram of calculated electromagnetic field distributions in entire BCS space to show the focusing ability of RMS and BCS. Dashed lines sketch the outline of RMS and BCS to show their location. We can find from Fig. 7 that the focusing ability of BCS is better than that of RMS. Simulation results over the frequency band 25 GHz–43 GHz are shown in Fig. 8. Fig. 8(a) shows the HPBW on the focal plane of BCS is less than 3.2 mm. Fig. 8(b) shows the HPBW is less than 8 mm at 25 GHz and less than 4 mm at 43 GHz on the $d = 4$ mm reception plane, and the first side lobe of the power distribution is less than 0.1. That is to say, the designed BCS can be applied over the Ka band 26.5 GHz–40 GHz to measure the permittivity or thickness variance of the dielectric plate from cell to cell with higher spatial resolution power. If the measurement is carried out in other frequency band such

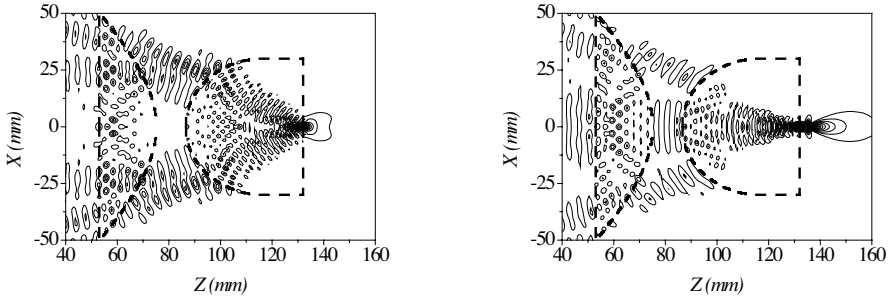

(a) RMS (b) BCS

Figure 7. Power distribution in the entire reception plane.

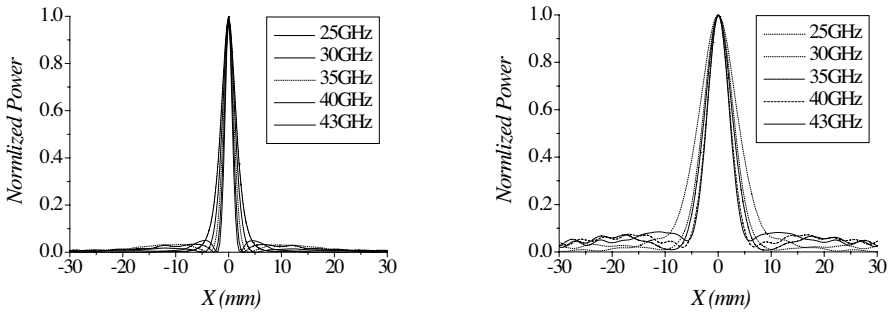

(a) Focal plane (*d=0mm*) (b) Reception plane (*d=4mm*)

Figure 8. Power distribution on the reception plane of BCS.

as W band, BCS has to be redesigned because the parameters of IMRS are related to the frequency.

3. EXPERIMENTS TO VERIFY THE VALIDITY OF THE BCS

An experiment set is built up to measure the beam width of the BCS and provide experimental verification for our proposal. The measurement system is shown in Fig. 9. In this measurement system, Teflon is taken to fabricate all the lenses of the BCS because Teflon is easier than Quartz for machining, that is, ε_{r2} listed in Fig. 3 is 2.1 instead of 3.78, which results in changes of set parameters: $S = 26.53\,\text{mm}$, $L = 20.70\,\text{mm}$ and $La = 3.91\,\text{mm}$. All the components of measurements set are fixed on the bracket which can be adjusted on an optical platform so as collimation is obtained. A standard

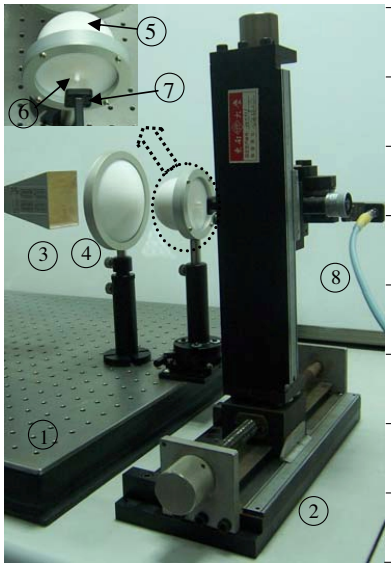

1	Optical measurement platform
2	2D adjustable set
3	Horn linked with signal generator
4	Hyperbolic lens
5	Extended hemispherical lens
6	Buncher lens
7	Receiving waveguide
8	Coaxial cable to spectrum analyzer

Figure 9. Measurement set of BCS.

gain horn with aperture size 69 mm × 57 mm in Ka band is used to radiate electromagnetic wave and a standard rectangular waveguide R320 fixed on a 2D adjustable bracket is used as a receiving component. Agilent signal generator E8257D and spectrum analyzer PSA447 are used in our measurements. The 2D adjustable bracket is adjusted carefully to make the receiving waveguide collimating to the buncher lens. The distance between the receiving waveguide and the buncher lens, which is corresponding to parameter d in Fig. 2, is estimated by a ruler between 1 mm and 2 mm. Shifting the bracket finely to change the receiving waveguide location relative to the buncher lens in the vertical and horizontal direction, recording the corresponding dB value displayed in the spectrum analyzer and the distribution of the electromagnetic energy will be obtained. Fig. 10 shows the normalized power distribution measured in dB. In order to compare it with the simulated results, the normalized power value measured in dB is converted to normalized absolute value as shown in Fig. 11. Here the simulated results are obtained by FDTD method. In simulation the incident wave impacting on the hyperbolic lens is the radiated wave by a horn, which is connected to a waveguide where TE10 mode is dominating mode. It is the same as the measurement set. Simulation results are given for $d = 1$ mm and $d = 2$ mm, then compared with measured results as shown in Fig. 11, good agreement have been

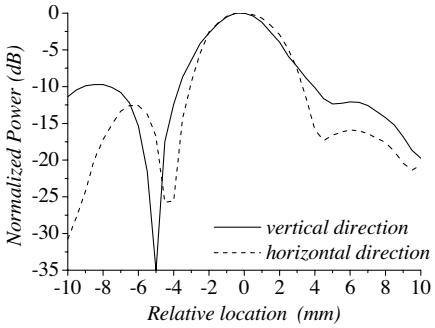

Figure 10. Power distribution measured on reception plane.

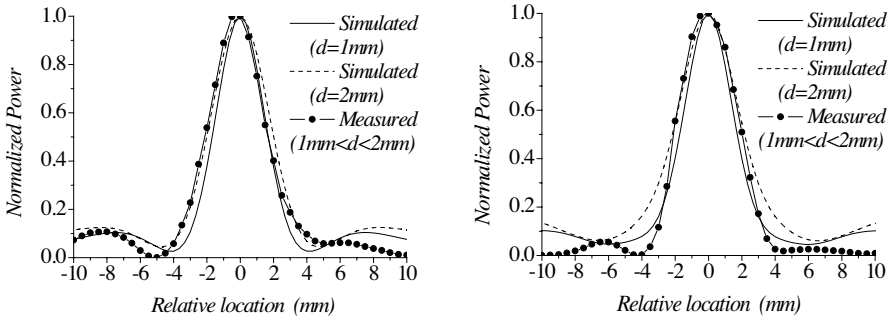

(a) Vertical direction (b) Horizontal direction

Figure 11. Comparison of simulated and measured power distribution.

observed. The HPBWs measured in vertical and horizontal direction are about 3.7 mm and 4.1 mm respectively, which are much less than the 10 mm HPBW of Gaussian beam on the beam waist plane, as we expected. The difference of normalized power distributions between vertical and horizontal direction may be from the different dimension of the receiving waveguide in both directions. Another measurement is also carried out for $2\,\text{mm} < d < 3\,\text{mm}$, again thin beam distribution is obtained and it is also agreement with the simulations.

In the BCS system, when the relative dielectric permittivity ε_{r2} of the extended hemispherical lens and buncher lens decreases, the HPBW of the BCS will increase, that is, the focusing ability of BCS will decrease as shown in Fig. 4(b) and Fig. 11. In the measurements, the collimation excursion of BCS and receiving waveguide and other offset will cause the asymmetry of the measured power distribution

along vertical or horizontal direction as shown in Fig. 10 and Fig. 11. In the measurement, the fabrication errors of lens geometrical parameters will also cause a little of variation of focusing property, we can adjust the distance between the lenses to achieve good performances.

4. NUMERICAL EXTRACTION TECHNIQUES

The reflection and transmission coefficients of an infinite uniform dielectric plate can be defined as [4]:

$$\Gamma_S = \frac{\Gamma\left(1-T^2\right)}{1-\Gamma^2T^2} \tag{1}$$

$$T_S = \frac{T\left(1-\Gamma^2\right)}{1-\Gamma^2T^2} \tag{2}$$

where:

$$\Gamma = \frac{1-\sqrt{\varepsilon_r}}{1+\sqrt{\varepsilon_r}} \tag{3}$$

$$T = \exp\left(-j\sqrt{\varepsilon_r}\frac{\omega}{c}t\right) \tag{4}$$

In (3) and (4), ε_r is the relative permittivity, t is the thickness of the sample, ω is the angular frequency and c is the light velocity.

Many techniques based on reflection and transmission coefficients were used to extract the dielectric constant in references [4, 26–29] etc. As shown in Fig. 2, the output wave of the BCS can behave as plane wave in a certain distance. If the reflection and transmission coefficients of the dielectric plate under test in our BCS equals to that of formulae ($1 \sim 4$), all the techniques based on reflection and transmission coefficients mentioned above can be used to accurately the thickness or permittivity of the sample as conventional free-space method. Simulations indicate that the reflection and transmission coefficients of the uniform dielectric plate obtained in BCS agree very well with that from formulae ($1 \sim 4$), as shown in Fig. 12 and Fig. 13. In Fig. 12, the relative permittivity of the dielectric plates is 3.78 (Quartz-glass), and in Fig. 13, the thickness of the dielectric plates is 2 mm. Fig. 12 and Fig. 13 indicate that when the thickness or permittivity of the sample under test varies, BCS and the formulae stated above give almost the same values of reflection and transmission coefficients. So the techniques based on reflection and transmission coefficients mentioned above can be used to extract the thickness or permittivity of the sample in our BCS. As shown in Fig. 13, when the

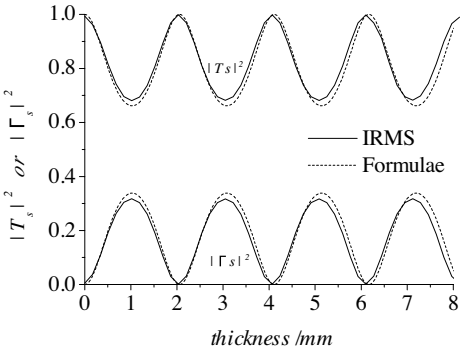

Figure 12. $|T_S|^2$ and $|\Gamma_S|^2$ variance with thickness.

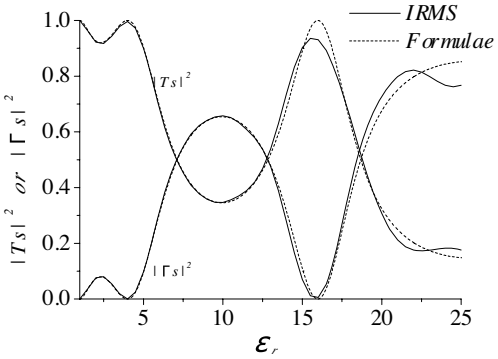

Figure 13. $|T_S|^2$ and $|\Gamma_S|^2$ variance with permittivity.

relative permittivity is higher than 15, the difference between curves obtained by formula ($1 \sim 4$) and our calculation enlarges. That is to say, if the sample relative permittivity is higher than 15, new technique has to be developed to extract the thickness or permittivity of the sample for our BCS. This work will be carried out in the future. Now we focus our attention on detecting the thickness or permittivity variance inhomogeneity and irregularity of dielectric plate with BCS' higher spatial resolution.

5. APPLICATION OF THE BCS IN MEASUREMENT SYSTEM

The BCS presented in this paper is attractive not only owing to its contactless and non-destructive nature, relative simplicity of sample

preparation, and suitability for high-frequency material measurement as other free-space methods, but also its higher spatial resolution. It can be used to identify the difference of dielectric material properties from cell to cell not only the permittivity but also the thickness variance of materials.

Figure 12 and Fig. 13 show that $|T_S|^2$ and $|\Gamma_S|^2$ change with the thickness d or the relative permittivity ε_r periodically. To elucidate the high spatial resolution of the BCS, the variable of the dielectric plate thickness and permittivity will be selected between the scope where $|T_S|^2$ and $|\Gamma_S|^2$ varied monotonically with the thickness or permittivity respectively. If the dielectric plate is shifted step by step, the $|T_S|^2$ or $|\Gamma_S|^2$ for different cell of the plate at each step will be obtained, then the property of the plate from cell to cell will be acquired.

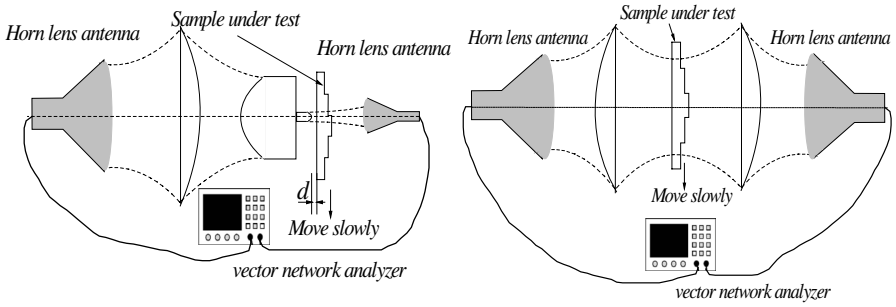

(a) BCS (b) Gaussian Beam

Figure 14. Configuration of BCS and Gaussian beam.

Figures 14(a) and (b) indicate the measurement set of BCS and a conventional free-space method using Gaussian beam [4]. The BCS measurement system consists of two horn lens antennas, BCS and a vector network analyzer, and the sample to be tested is placed after BCS as shown in Fig. 14(a). The BCS creates a quasi-plane wave at the sample location, which allows plane wave theory to be used in the calculations. The Gaussian beam measurement system consists of a pair of collinear horn-fed lenses, two horn lens antennas and a vector network analyzer, and the sample to be tested is inserted midway between the two lenses as shown in Fig. 14(b). The horn-fed lenses create a Gaussian plane wave at the sample location and plane wave theory is allowed in the calculations. In both measurement systems, if we move the dielectric plate step-by-step and record the reflection or transmission coefficients of different cell of the plate at each step by the network analyzer, the reflection and transmission coefficients distribution of the plate can be obtained. Once the reflection and

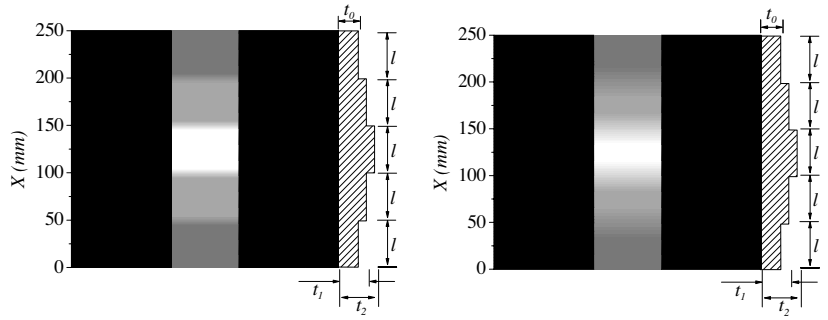

Figure 15. Images of medium plate with different thickness.

transmission coefficients are calibrated, they may be used to extract the thickness or permittivity. So the thickness or permittivity distribution of the dielectric plate can be obtained.

5.1. Imaging of Thickness

The BCS can be used to measure the thickness of materials. As shown in Fig. 14, by shifting the dielectric plate step-by-step and recording transmission coefficients at each step for different cell of the plate, the image of the thickness could be obtained by constructing the gray scale map of the transmission coefficients $|T_S|^2$ value, and the brightness of the image is corresponding to the thickness of the plate. In our simulations, according to Fig. 12, we select the plate thicknesses of 1.0 mm, 1.4 mm and 1.8 mm, which are located between the monotone intervals. Fig. 15 is the image of an irregular dielectric plate with different thickness. The parameters of the dielectric plate are shown in Fig. 15, where $t_0 = 1.0\,\text{mm}$, $t_1 = 1.4\,\text{mm}$, $t_2 = 1.8\,\text{mm}$, $l = 50\,\text{mm}$, and the permittivity is 2.1 (Teflon). Fig. 15(a) is obtained by BCS, while (b) is obtained by the conventional Gaussian beam method. In our simulation, the shift step is 0.1 mm. All the simulations are performed at 37.5 GHz, which corresponds to a free-space wavelength of 8 mm. It can be seen that the thickness discontinuity of the dielectric plate in Fig. 15(a) is clearer than that in Fig. 15(b). That is to say, the clear image from cell to cell results from the higher spatial resolution of BCS.

5.2. Imaging of Permittivity

The BCS can also be used to measure the permittivity variance of dielectric materials. Using the method above, the images of medium

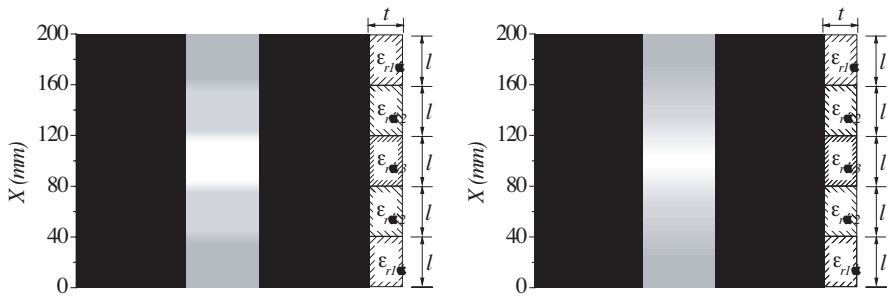

Figure 16. Image of medium plate with different permittivity.

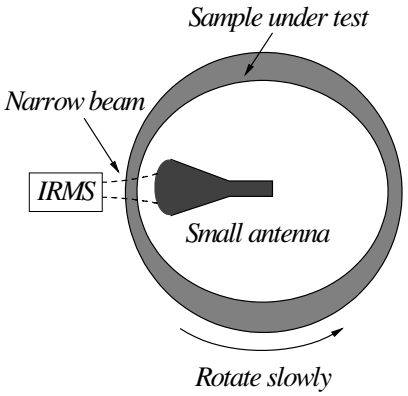

Figure 17. Diagrammatic sketch of measuring irregular medium.

plate with different permittivity can be obtained too. Fig. 16 shows the image of a medium plate with different permittivity. The parameters of the medium plate are shown in Fig. 16, where $t = 2.2\,\text{mm}$, $l = 40\,\text{mm}$ and the relative permittivity $\varepsilon_1 = 4.7$, $\varepsilon_2 = 4.6$, $\varepsilon_3 = 4.5$, which are located between the monotone intervals in Fig. 13. Fig. 16(a) is obtained by the BCS method stated above, while (b) is obtained by the conventional Gaussian beam method. In the measurement simulations, the shift step is 0.1 mm. The simulations are also performed at 37.5 GHz. As shown that Fig. 16(b) are not as clear as Fig. 16(a). That is to say, the spatial resolution of BCS is higher than that of conventional Gaussian beam method.

As show in Fig. 15 and Fig. 16, BCS can show the variation of permittivity or thickness of dielectric plate more sharply than the Gaussian beam method. Furthermore, non planar shaped material

such as cylinder sleeve as shown in Fig. 17, which could not be easily measured by the traditional free space or open cavity method, can also be measured conveniently by the BCS presented in this paper because of the small size of the receiving antenna.

6. CONCLUSION

A beam compressed system (BCS) is proposed and verified by experiments in this paper. It is attractive not only owing to its contactless and non-destructive nature, relative simplicity of sample preparation, and suitability for high-frequency material measurement as other free-space methods, but also its higher spatial resolution power and low cost. Images of materials with different thickness and permittivity have been depicted. Sharply defined images of the material property have been presented to show the advantages of BCS over conventional free space method. Further study will be focused on the permittivity and thickness extraction technique. that will be presented in next paper.

ACKNOWLEDGMENT

This work is supported by NSFC (60571028) and the support is genuinely and sincerely appreciated.

REFERENCES

1. Afsar, M. N. and H. Ding, "A novel open-resonator system for precise measurement of permittivity and loss-tangent," *IEEE Trans. Instrum. Meas.*, Vol. 50, 402–405, 2001.
2. Shimabukuro, F. I., S. Lazar, M. R. Chernick, and H. B. Dyson, "A quasi-optical method for measuring the complex permittivity of materials," *IEEE Trans. Microwave Theory Tech.*, Vol. 32, 659–665, 1984.
3. Ghodgaonkar, D. K., V. V. Varadan, and V. K. Varadan, "A free-space method for measurement of dielectric constants and loss tangents at microwave frequencies," *IEEE Trans. Instrum. Meas.*, Vol. 37, 789–793, 1989.
4. Gagnon, N., J. Shaker, et al., "Low-cost free-space measurement of dielectric constant at Ka band," *IEE Proc. - Microw. Antennas Propag.*, Vol. 151, 271–276, 2004.
5. Hollinger, R. D., K. A. Jose, A. Tellakula, V. V. Varadan, and V. K. Varadan, "Microwave characterization of dielectric

materials from 8 to 110 GHz using a free-space setup," *Microw. Opt. Technol. Lett.*, Vol. 26, 100–105, 2000.

6. Biju Kumar, J., U. Raveendranath, et al., "A simple free-space method for measuring the complex permittivity of single and compound dielectric materials," *Microw. Opt. Technol. Lett.*, Vol. 26, 117–119, 2000.
7. Qian, C. and W. B. Dou, "A new approach for measuring permittivity of dielctric material," *J. of Electromagn. Waves and Appl.*, Vol. 19, No. 6, 795–810, 2005.
8. Dou, W. B., *Millimeter Wave Quasi-Optical Theory and Technology*, Publishing House of Electronics Industry, Beijing, China, 2000 (in Chinese).
9. Kume, E. and S. Sakai, "Properties of a dielectric probe for scanning near-field millimeter-wave microscopy," *Journal of Applied Physics*, Vol. 99, 056105, 2006.
10. Rosner, B. T. and D. W. van der Weide, "High-frequency near-field microscopy," *Review of Scientific Instruments*, Vol. 73, No. 7, 2505–2525, 2002.
11. Kharkovsky, S. and R. Zoughi, "Microwave and millimeter wave nondestructive testing and evaluation: Overview and recent advances," *IEEE Instrumentation & Measurement Magazine*, Vol. 10, 26–38, 2007.
12. Anlage, S. M., V. V. Talanov, and A. R. Schwartz, *Scanning Probe Microscopy: Electrical and Electromechanical Phenomena at the Nanoscale*, 215–253, Springer, New York, 2007.
13. Chala, R. K., D. Kajfez, et al., "Permittivity measurement with a non-standard waveguide by using TRL calibration and fractional linear data filtering," *Progress In Electromagnetics Research B*, Vol. 2, 1–13, 2008.
14. An, G. and W. B. Dou, "Analysis of sphere lens quasi-optical monopulse-antenna/feed structure," *J. of Electromagn. Waves and Appl.*, Vol. 19, No. 1, 83–93, 2005.
15. Wang, Z. X. and W. B. Dou, "Design and analysis of several kinds of dielectric lens antennas," *J. of Electromang. Waves and Appl.*, Vol. 20, No. 12, 1643–1653, 2006.
16. Tuz, V., "Three-dimensional scattering of Gaussian beam from a periodic sequence of bi-isotropic and material layers," *Progress In Electromagnetics Research B*, Vol. 7, 53–73, 2008.
17. Wang, M.-J., Z.-S. Wu, and Y.-L. Li, "Investigation of scattering characteristics of Gaussian beam from two dimensional dielectric rough surfaces based on the Kirchhoff approximation," *Progress*

In Electromagnetics Research B, Vol. 4, 223–235, 2008.

18. Huang, C.-H., Y.-F. Chen, and C. C. Chiu, "Permittivity distribution reconstruction of dielectric object by a cascaded method," *J. of Electromang. Waves and Appl.*, Vol. 21, No. 2, 145–159, 2007.
19. Liao, S.-L. and R. J. Vernon, "Sub-THz beam-beam-shaping mirror system designs for quasi-optical mode converters in high-power gyrotrons," *J. of Electromagnetic Waves and Appl.*, Vol. 21, No. 4, 425–439, 2007.
20. Yin, H. P. and W. B. Dou, "Analysis of an extended hemi-spherical lens antenna at millimeter wavelengths," *J. of Electromagn. Waves and Appl.*, Vol. 16, No. 9, 1209–1222, 2002.
21. Mei, Z. L. and W. B. Dou, "Performances of hyperbolical and spherical lens imaging systems at millimeter wavelengths," *J. of Electromagn. Waves and Appl.*, Vol. 16, No. 8, 1077–1093, 2002.
22. Rutledge, D. B. and M. S. Muha, "Imaging antenna arrays," *IEEE Trans. AP*, Vol. 30, 535–540, 1982.
23. Dou, W. B., X. D. Deng, and J. H. Pan, "Analysis of extending the field-of-view of reverse-microscope imaging system at millimeter-wavelengths," *Journal of Electromagnetic Waves and Applications*, Vol. 18, 469–479, 2004.
24. Allen, T., *Computational Electrodynamics: The Finite-Difference Time-Domain Method*, Artech House, 2000.
25. Jin, J.-M., *The Finite Element Method in Electromagnetics*, John Wiley, 2002.
26. Nicolson, A. M. and G. Ross, "Measurement of intrinsic properties of materials by time domain techniques," *IEEE Trans. Instrum. Meas.*, Vol. 19, 377–382, 1970.
27. Weir, W. B., "Automatic measurement of complex dielectric constant and permeability at microwave frequencies," *Proc. IEEE*, Vol. 62, 33–36, 1974.
28. Boughriet, A. H., C. Legrand, and A. Chapoton, "Noniterative stable transmission/reflection method for low-loss material complex permittivity determination," *IEEE Trans. Microwave Theory Tech.*, Vol. 245, 52–57, 1997.
29. Baker-Jarvis, J., E. J. Vanzura, and W. A. Kissick, "Improved technique for determining complex permittivity with the transmission/reflection method," *IEEE Trans. Microwave Theory Tech.*, Vol. 38, 1096–1103, 1990.